Technobius Physics, 2023, 1(4), 0005, DOI: https://doi.org/10.54355/tbusphys/1.4.2023.0005

Technobius Physics

https://technobius.kz/

e-ISSN 3007-0147

Corrigendum Notice: A corrigendum has been issued for this article and is included at the end of this document.

Article

Exploring the labyrinth of light: multiple Bragg Diffraction phenomena in face-centered cubic photonic crystals

Nurzhan Dosaev, Gulzhan Tulekova*

Physics Department, M. Kozbayev North Kazakhstan University, 13 Internatsionalnaya str., Petropavlovsk, Kazakhstan
*Correspondence: gulzhan.tulekova@bk.ru

Abstract. This work presents the outcomes of an experimental study aimed at exploring electron diffraction phenomena within a controlled environment. The experiment involved measuring the radii of diffraction rings produced under varying acceleration voltages, with a focus on the first-order ring. Unexpectedly, the observed values were half of the anticipated results, raising questions about the accuracy of the measurements. The analysis revealed that the measured value of d_1 closely resembled the theoretical value of d_2, suggesting a potential oversight of the first diffraction ring, possibly due to its diminutive size. The high brightness of the incident light further complicated the measurement process. Accounting for the possibility of overlooking the first diffraction ring, the derived values for d_2 (128.24±33.26 pm) and d_3 (70.00±5.21 pm) were compared to theoretical values (123 pm and 80 pm, respectively). Despite the challenges, the experimental results fell within an acceptable range, considering the inherent uncertainties. To mitigate errors in radii measurement, the article suggests the implementation of an automated system and recommends a thorough reassessment of experimental setup configurations to optimize conditions for more accurate measurements. The findings highlight the importance of methodological refinement to enhance precision and reliability in electron diffraction studies. This work contributes valuable insights to the field and underscores the continuous need for advancements in experimental techniques.
Keywords: photonic crystals, crystallography, face-centered cubic, diffraction phenomena, labyrinth of light.

1. Introduction

Bragg's law elucidates the relationship between the wavelength of incident radiation and the angle at which it is scattered by lattice planes, resulting from the constructive interference of wave fronts [1]. The phenomenon of Bragg diffraction contributes to the emergence of band gaps within the energy spectra of diverse periodic structures. Among these structures are photonic crystals (PhCs) [1–4], characterized by band gaps within the electromagnetic spectrum. The position of these gap energies is determined by the periodic modulation of the dielectric constant [1-4].

In the context of light Bragg diffraction, understanding the processes occurring at the surface of the Brillouin zone (BZ) where photonic stop bands emerge is crucial. Bragg diffraction manifests when the Laue conditions are met: $k_s=k_i+g_{hkl}$, where k_s and k_i represent the wave vectors of the incident and scattered light waves, respectively, g_{hkl} indeed determined by a system of scattering planes with Miller indices (hkl) [1-4].

Scientists have established that the quality of graphite is primarily characterized by its carbon content and structural properties [5]. Unlike a single crystal, graphite does not exist as a single mineral formation; it predominantly exists in the form of aggregates consisting of graphite and its enrichment products. In addition, various structure less carbon phases may be present along with graphite. The properties of these materials are influenced not only by the carbon content, but also by the amount and arrangement of crystalline, or ordered, graphite - in essence, the texture and structure of the material. Therefore, to accurately assess the properties of graphite samples, it is necessary to consider both their crystal structure and the texture and structure of all components present [5-9].

The research team published a paper [10] that displayed the effects observed when soft carbon materials undergo annealing at high temperatures or when graphite is subjected to disordered-inducing processes such as fast neutron irradiation or mechanical grinding.

X-ray structural analysis is commonly employed to explore the crystalline arrangement of carbon materials like graphite [11]. This method allows for the assessment of the structure's level of organization and the dimensions of its crystallites, which are the smallest building blocks of the structure. The composite data collected from diverse sources indicates characteristic interlayer spacings at approximately 3.38 Å, 3.40 Å, 3.425 Å, 3.44 Å, and 3.55 Å, along with one notably observed around 3.68 Å [11–12].

In this paper, the lattice properties of graphite were studied in detail using X-ray irradiation. The X-ray irradiation method provided information about the structure of graphite and its characteristics.

2. Methods

The experiment investigates the wave-particle duality of electrons through the diffraction of fast electrons by a polycrystalline graphite layer, a phenomenon analogous to the diffraction of light. As the electrons interact with the graphite crystal lattice, they exhibit wave-like behavior, generating interference patterns in the form of concentric rings on a fluorescent screen [10–12]. The primary objective of the experiment is to measure the diameter of these diffraction rings at various accelerating voltages to determine the interplanar spacing within the graphite structure. By applying the principles of electron diffraction and Bragg's law, the interplanar spacings are calculated using the observed ring diameters and the known accelerating voltages [10–12]. This experiment thus serves to elucidate the fundamental properties of crystal structures and to reinforce the dual nature of electrons as both particles and waves.

The electron diffraction apparatus is a comprehensive assembly designed to probe the wave-particle duality of electrons via their interaction with a crystalline structure. Central to this setup is the Electron Diffraction Tube, meticulously mounted to ensure the precise trajectory of electrons towards the target polycrystalline graphite layer. This tube is the heart of the experiment, where the crucial phenomenon of electron diffraction occurs.

To facilitate the acceleration of electrons to the requisite high speeds, a High Voltage Supply Unit is employed, capable of delivering an adjustable voltage ranging from 0 to 10 kV. The flow of electrons is carefully regulated by a 10 MOhm High-value Resistor, which serves to limit the current and provide an additional layer of safety against electrical surges.

The intricate connections within the apparatus are made possible by specialized Connecting Cords rated for 50 kV, with a standard length of 500 mm, ensuring safe transmission of high voltage to the diffraction tube. Additionally, a separate Power Supply unit, adjustable up to 600 V, is utilized for precise control over the electron beam and to power ancillary components of the setup.

Measurements of the resulting diffraction patterns are taken with a Vernier Caliper made of plastic, chosen for its non-conductive properties, which is essential for maintaining safety in an environment where high voltages are present. The caliper's precision allows for accurate determination of the ring diameters, which are pivotal for calculating the interplanar spacings in the graphite lattice.

The apparatus also includes an assortment of Connecting Cords in various lengths—250 mm and 750 mm—and colors—red, blue, yellow, and black. These cords not only facilitate a secure and organized connection between the various components but also adhere to standard color coding practices to aid in the correct setup. Red and blue cords typically denote positive and negative connections, respectively, while yellow and black cords are used for grounding or common connections. All provided equipments are manufactured by the SciTech Company, USA.

Together, these components form a sophisticated system that, when correctly assembled and calibrated, enables the detailed study of electron diffraction patterns. The careful design and selection

of each element ensure that the apparatus functions safely and effectively, providing valuable insights into the quantum nature of electron behavior and the structural properties of crystalline materials.

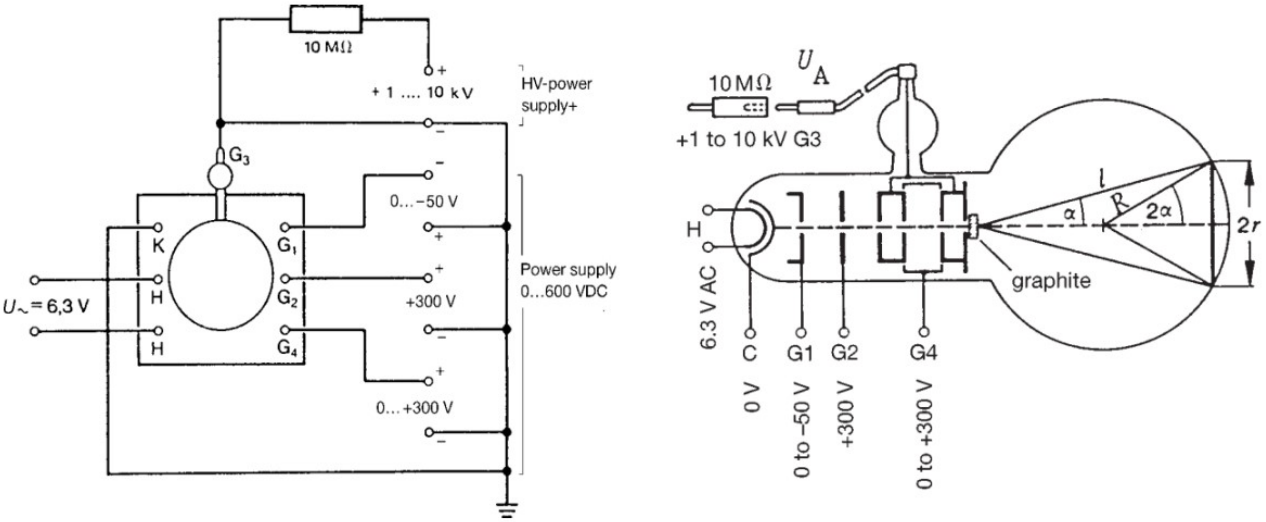

Figure 1 – Schematic diagram of the o the electron diffraction tube

The experimental apparatus was arranged in accordance with the schematic representation depicted in Figure 1. The electron diffraction tube was integrated into the experimental setup, with its sockets meticulously connected to the power supply following the configuration illustrated in Fig. 2. Notably, a secure connection was established between the high voltage and the anode G3 through a 10 MΩ protective resistor.

To ensure optimal diffraction outcomes, precise adjustments were made to the Wehnelt voltage G1, as well as the voltages G4 and G3. These adjustments were meticulously calibrated to elicit the formation of sharp and well-defined diffraction rings. The resultant diffraction pattern was subjected to analysis for further insights into the underlying electron behavior.

An essential step in the experimentation process involved reading the anode voltage directly from the display of the high-voltage power supply. This voltage measurement served as a critical parameter for subsequent analyses and interpretations.

All data were tabulated using Microsoft Excel 365. Diffraction ring diameters were used to calculate interplanar spacings via Bragg's law:

$$n\lambda = 2d \sin\theta \tag{1}$$

where $\lambda = \frac{h}{\sqrt{2meV}}$ is the de Broglie wavelength for electrons accelerated by voltage V, d is the spacing between lattice planes, and θ is the diffraction angle. The distance L between the target and screen was used to relate the ring diameter D to θ through:

$$\sin\theta \approx \frac{D}{2L} \tag{2}$$

For each voltage, ring diameter measurements were averaged and reported as mean ± standard deviation. A linear regression analysis of $1/D^2$ versus accelerating voltage V was performed to assess linearity, in accordance with theoretical predictions [3]. Analysis of variance (ANOVA) was used to determine whether differences between ring sizes across voltages were statistically significant (α = 0.05). All statistical calculations were performed in MATLAB R2021a.

In order to ascertain the dimensions of the diffraction rings, careful measurements were conducted using a Vernier caliper. In a controlled, darkened room environment, both the inner and outer edges of the diffraction rings were meticulously measured, and the obtained values were used to compute an average diameter. It is important to note the presence of an additional faint ring, situated immediately behind the second ring, highlighting the complexity of the diffraction pattern and the need for comprehensive analysis. This experimental approach adheres to established protocols

in electron diffraction studies, ensuring precision and reliability in the acquisition of data and subsequent interpretations.

3. Results and Discussion

The interference phenomenon observed in electron diffraction experiments can be explained through the concept of wave-particle duality, which is a cornerstone of quantum mechanics [15–16]. According to this concept, particles such as electrons exhibit both particle-like and wave-like properties. When electrons pass through a crystalline structure, they interfere with each other in a manner similar to waves, creating a pattern of constructive and destructive interference that can be observed and measured.

The electron diffraction experiment was conducted within a glass bulb with a specified radius of 65 mm. The diffraction patterns for the first-order ring were observed and measured across varying voltages, yielding data as presented in Tables 1 and 2. Table 1 provides diameter measurements for the first-order ring at voltages ranging from 4.0 kV to 6.5 kV.

Table 1 – Voltage levels ranging from 4.0 kV to 6.5 kV and corresponding measurements of the first-order ring's diameter

Voltage V, *kV*	Inner Diameter, ±0.05 *mm*	Outer Diameter, ±0.05 *mm*
4.0	28.78	36.51
	50.15	61.11
4.5	21.03	30.98
	46.74	55.48
5.0	24.68	30.28
	42.75	50.12
5.5	22.31	27.73
	41.02	46.13
6.0	21.34	24.97
	38.12	43.88
6.5	21.01	24.75
	35.14	42.02

It is imperative to note that the diameter measurements were obtained using a Vernier caliper in a controlled environment. The precision of the measurements, coupled with the systematic variation of voltage, provides a comprehensive dataset for the analysis of electron diffraction behavior within the specified experimental setup.

Table 2 – Voltage levels ranging from 7.0 kV to 9.9 kV and corresponding measurements of the first-order ring's diameter

Voltage V, *kV*	Inner Diameter, ±0.05 *mm*	Outer Diameter, ±0.05 *mm*
7.0	19.47	25.02
	34.05	39.15
7.5	19.04	20.14
	32.38	36.75
8.0	17.15	19.46
	31.13	35.38
8.5	17.41	19.06
	31.14	34.98
9.0	17.11	20.05
	28.72	33.45
9.5	16.63	17.65
	26.98	32.15
9.9	16.75	18.15
	27.03	30.03

The calculated wavelength is crucial for understanding the interference patterns observed in the experiment, as it allows for the application of Bragg's law to determine the interplanar spacing of the crystalline structure being used. In the described experiment, a diffraction tube along with the requisite equipment was utilized to explore the wave-like characteristics of particles, specifically electrons. The experiment hinged on the principle of electron diffraction, where electrons demonstrate wave behavior when passed through a crystalline structure, such as graphite.

Each entry includes both inner and outer diameter values, with a precision of ±0.05 mm. Notable variations in diameter are observed with changes in voltage, indicating the sensitivity of the diffraction pattern to applied electrical potentials. Similarly, Table 2 details diameter measurements for the first-order ring at higher voltages, ranging from 7.0 kV to 9.9 kV. The precision of ±0.05 mm is maintained for both inner and outer diameter values. Again, the data underscores the impact of increased voltage on the dimensions of the diffraction ring.

Table 3 – The wavelength of the electrons under a certain acceleration voltage

Voltage U_A, *kV*	Wavelength, *pm*	The error of wavelength, *pm*
4.0	19.19	0.127
4.5	18.18	0.130
5.0	17.34	0.114
5.5	16.53	0.113
6.0	15.76	0.110
6.5	15.14	0.106
7.0	15.03	0.103
7.5	15.16	0.098
8.0	13.72	0.097
8.5	13.28	0.096
9.0	13.03	0.085
9.5	12.51	0.081
9.9	12.34	0.077

The dataset reveals a consistent trend wherein as the acceleration voltage increases, the electron wavelength decreases. This relationship is pivotal for understanding the behavior of electrons under varying electrical potentials. The associated error values underscore the meticulous nature of the measurements, ensuring the accuracy of the reported electron wavelengths.

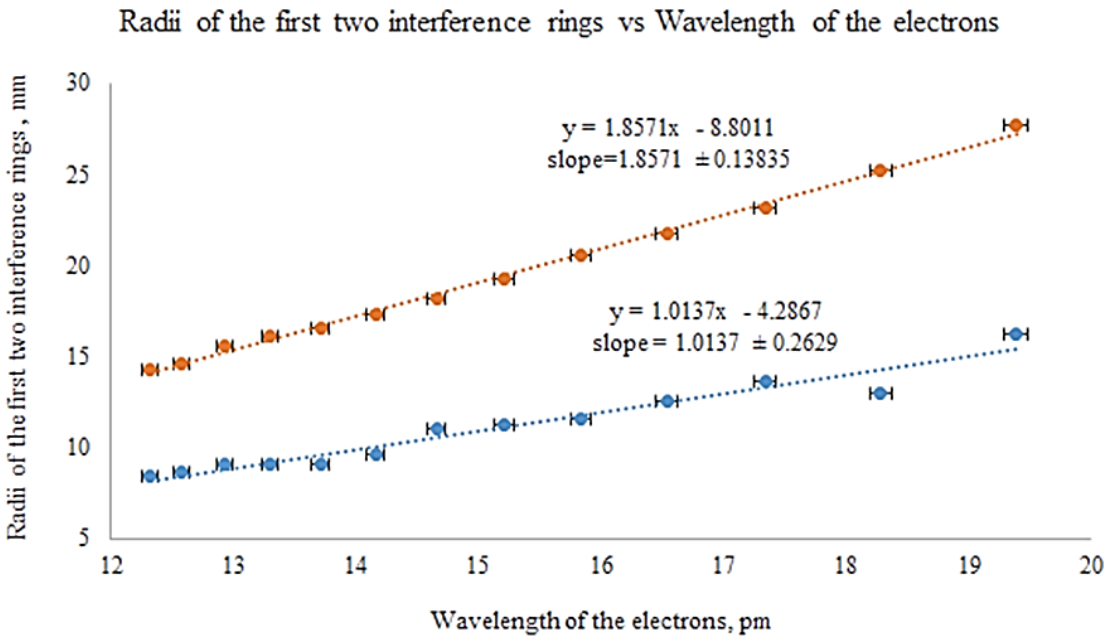

Figure 2 – Diameters of the initial two diffraction rings compared to the electron wavelength

These findings contribute to the broader comprehension of electron dynamics and wave-particle duality within the experimental framework.

The wavelength data, coupled with the associated errors, serves as a valuable resource for further analysis, theoretical modeling, and the advancement of knowledge in the field of electron diffraction studies.

As it can be seen, we observed some sort of unexpected results. We got values half as much as expected. Furthermore, according to the results of this experiment, the value of d_1 is closer to the theoretical value of d_2 and the value of d_2 is closer to the theoretical value of d_3. We obtained results as if we were measuring the radii of second and third visible diffraction rings. It might be possible if the first ring was much smaller than the second and the third rings.

The brightness of incident light could have potentially worsened the situation so that we could not clearly see the first diffraction ring.

If we treat the experimental value of d_1 as the theoretical value of d_2 and the experimental value of d_2 as the theoretical value of d_3, we can conclude that the experiment was conducted successfully. However, the error of d_1 is comparable with the calculated value.

This is because data points for d1 are not within the desired margin so that they would have a good linear fit with a small slope error. It possibly might have been the result of systematic error in measuring diffraction rings' radii because those diffraction rings have very blurry boundaries and precisely measuring the inner and outer radii of the first diffraction ring is difficult for small values. This explains why d1 has a greater error than d_2.

We can mitigate the issue with radii measuring if we will use a sort of automatic measuring system that would easily measure inner and outer radii without cognitive biases that humans have. Also changing configurations so that diffraction rings are easier to measure can improve the situation with the error of d_1.

4. Conclusions

In a broader context, the success of the experiment hinges on the assumption that the measured parameters correspond to interplanar spacings d_2 and d_3, while the diffraction ring associated with d1 may have been sufficiently small to escape detection. The heightened brightness of the incident light potentially exacerbated this situation. Considering the possibility of overlooking the first diffraction ring, the derived values suggest that d_2 is 128.24±33.26 pm and d_3 is 70.00±5.21 pm. In comparison, the theoretical values for d_2 and d_3 are 123 pm and 80 pm, respectively. Remarkably, the experiment's results fall within an acceptable range, considering the inherent uncertainties.

To address the error in measuring diffraction ring radii, implementing an automated system is recommended, offering a potential solution by minimizing human-induced biases. Additionally, a careful reassessment and optimization of the experimental setup configurations are essential. Identifying ideal conditions under which diffraction rings are more easily measurable can significantly enhance the precision and reliability of the experimental outcomes. These considerations underscore the continuous need for refinement in methodology to ensure the accuracy of results and contribute to the advancement of scientific knowledge in the field.

References

1. Multiple Bragg diffraction in opal-based photonic crystals: Spectral and spatial dispersion / I.I. Shishkin, M.V. Rybin, K.B. Samusev, V.G. Golubev, M.F. Limonov // Physical Review B. — 2014. — Vol. 89. — P. 035124. https://doi.org/10.1103/PhysRevB.89.035124
2. Photonic Crystals: Molding the Flow of Light / J.D. Joannopoulos, S.G. Johnson, J.N. Winn, R.D. Meade. — Princeton, USA: Princeton University Press, 2018. — 305 p.
3. Optical Properties of Photonic Crystals / K. Sakoda. — New York, USA: Springer, 2004. — 258 p.
4. Optical Properties of Photonic Structures: Interplay of Order and Disorder / M.F. Limonov, R.M. De La Rue. — Florida, USA: CRC Press, Taylor & Francis Group, 2012. — 528 p.
5. Crystallographic Analysis of Graphite by X-Ray Diffraction / A.N. Popova // Chemistry. — 2017. — Vol. 60. No. 9. — P. 361-365. https://doi.org/10.3103/S1068364X17090058

6. Photonic band gaps structure properties of two-dimensional function photonic crystals / J. Lachter, R.H. Bragg // Physical Review B. — 2017. — Vol. 89. — P. 61 – 66. https://doi.org/10.1016/j.physe.2017.01.028
7. XRD Characterization of the Structure of Graphites and Carbon Materials Obtained by the Low-Temperature Graphitization of Coal Tar Pitch / Ch.N. Barnakov, G.P. Khokhlova, A.N. Popova, S.A. Sozinov, Z.R. Ismagilov // Eurasian Chemico-Technological Journal. — 2015. — Vol. 17. — P. 87–93.
8. Photonic Crystals: Molding the Flow of Light / J.D. Joannopoulos, S.G. Johnson, J.N. Winn, R.D. Meade. — Princeton, USA: Princeton University Press, 2008. — 305 p.
9. Inhibited spontaneous emission of quantum dots observed in a 3D photonic band gap / M.D. Leistikow, A.P. Mosk, E. Yeganegi, S.R. Huisman, A. Lagendijk, W.L. Vos // Physical Review Letters. — 2011. — Vol. 107, No. 19. — P. 193903. https://doi.org/10.1103/PhysRevLett.107.193903
10. Observation of sub-Bragg diffraction of waves in crystals / S.R. Huisman, R.V. Nair, A. Hartsuiker, L.A. Woldering, A.P. Mosk, W.L. Vos // Physical Review Letters. — 2012. — Vol. 108, No. 8. — P. 083901. https://doi.org/10.1103/PhysRevLett.108.083901
11. Diffraction of light from thin-film polymethyl methacrylate opaline photonic crystals / S. G. Romanov et al // Physical Review Letters. — 2001. — Vol. 63, No. 5. — P. 056603. https://doi.org/10.1103/PhysRevE.63.056603
12. Polarized light coupling to thin silica-air opal films grown by vertical deposition / A. V. Baryshev et al. // Physical Review Letters. — 2007. — Vol. 76, No. 1. — P. 014305. https://doi.org/10.1103/PhysRevB.76.014305

Information about authors:

Nurzhan Dosaev – Master Student, Physics Department, M. Kozbayev North Kazakhstan University, 13 Internatsionalnaya str., Petropavlovsk, Kazakhstan, dosayev.n@gamil.com
Gulzhan Tulekova – Master Student, Physics Department, M. Kozbayev North Kazakhstan University, 13 Internatsionalnaya str., Petropavlovsk, Kazakhstan, gulzhan.tulekova@bk.ru

Author Contributions:

Nurzhan Dosaev – concept, methodology, data collection, analysis, visualization, drafting.
Gulzhan Tulekova – resources, testing, modeling, interpretation, editing, funding acquisition.

Received: 8 September 2023
Revised: 25 September 2023
Accepted: 28 September 2023
Published: 28 September 2023